J Oceanogr (2014) 70:415–424
DOI 10.1007/s10872-014-0241-9

ORIGINAL ARTICLE

Application of chemical tracers to an estimate of benthic denitrification in the Okhotsk Sea

Masanori Ito · Yutaka W. Watanabe · Masahito Shigemitsu · Shinichi S. Tanaka · Jun Nishioka

Received: 27 October 2013 / Revised: 20 June 2014 / Accepted: 7 August 2014 / Published online: 24 August 2014
© The Oceanographic Society of Japan and Springer Japan 2014

Abstract To estimate benthic denitrification in a marginal sea, we assessed the usefulness of N_2^*, a new tracer to measure the excess nitrogen gas (N_2) using dissolved N_2 and argon (Ar) with N^* in the intermediate layer (26.6–27.4σ_θ) of the Okhotsk Sea. The examined parameters capable of affecting N_2^* are denitrification, air injection and rapid cooling. We investigated the relative proportions of these effects on N_2^* using multiple linear regression analysis. The best model included two examined parameters of denitrification and air injection based on the Akaike information criterion as a measure of the model fit to data. More than 80 % of N_2^* was derived from the denitrification, followed by air injection. Denitrification over the Okhotsk Sea shelf region was estimated to be 5.6 ± 2.4 μmol kg^{-1}. The distribution of N_2^* was correlated with potential temperature (θ) between 26.6 and 27.4σ_θ ($r = -0.55$). Therefore, we concluded that N_2^* and N^* can act complementarily as a quasi-conservative tracer of benthic denitrification in the Okhotsk Sea. Our findings suggest that N_2^* in combination with N^* is a useful chemical tracer to estimate benthic denitrification in a marginal sea.

Keywords Benthic denitrification · The marginal sea · The Okhotsk Sea · Chemical tracer · Multiple linear regression analysis

M. Ito (✉) · Y. W. Watanabe
Graduate School of Environmental Science, Hokkaido University, Sapporo, Japan
e-mail: masaito@ees.hokudai.ac.jp

Y. W. Watanabe · M. Shigemitsu
Faculty of Earth Environmental Science, Hokkaido University, Sapporo, Japan

S. S. Tanaka
Earthquake Research Institute, The University of Tokyo, Tokyo, Japan

J. Nishioka
Institute of Low Temperature Science, Hokkaido University, Sapporo, Japan

1 Introduction

The marine fixed nitrogen (N) cycle is highly dynamic because of large input-output rates and a shorter turnover time compared to the cycles of other biologically important nutrients. Despite recent developments in our understanding of the processes and magnitude of the pathways in the marine N cycle, a number of open questions remain (Brandes et al. 2007). Denitrification in the water column and sediments, including canonical denitrification and anaerobic ammonium oxidation (anammox), is the primary sink of N from fixed forms to molecular nitrogen (N_2) (Brandes et al. 2007; Eugster and Gruber 2012). Conversely, N_2 fixation by diazotrophs is the major oceanic source of biologically available N in the open ocean (Galloway et al. 2004). In particular, there is controversial disagreement as to how close the marine N cycle is balanced between N_2 fixation and denitrification (Codispoti 2007; Codispoti et al. 2001; Codispoti and Christensen 1985; Gruber 2004; Gruber and Sarmiento 1997).

Denitrification occurs primarily in continental marginal sediments (Christensen et al. 1987; Middelburg et al. 1996) and in the three major oxygen-deficient zones (ODZs) that experience oxygen concentrations less than 4 μmol kg^{-1}: the eastern tropical North and South Pacific and the Arabian Sea (Codispoti et al. 2001; Codispoti and Christensen 1985; Codispoti et al. 2005). While reports related to

nitrogen sources and sinks have increased over the past 20 years, estimation of benthic denitrification is the most poorly constrained (Codispoti 2007; DeVries et al. 2012; Liu and Kaplan 1984; Middelburg et al. 1996).

There are several ways to constrain the biologically available marine N budget in the global ocean (Codispoti 2007; Gruber and Sarmiento 1997). For example, Gruber and Sarmiento (1997) proposed a quasi-conservative tracer N^* (=([NO_3^-] − 16[PO_4^{3-}] + 2.9) × 0.87) as an index of N_2 fixation-denitrification using the observed nutrient data. In general, N^* increases with N_2 fixation because diazotrophs fix N_2 into the internal nitrogen cycle in the ocean, and it decreases with denitrification because microbes consume nitrate. However, the distribution of N^* may reflect not only N_2 fixation and denitrification, but also other important processes. Such processes include variable phytoplankton stoichiometry (Weber and Deutsch 2010), atmospheric deposition (Hansell et al. 2007) and different remineralization rates for total organic phosphorus and nitrogen (Coles and Hood 2007; Landolfi et al. 2008; Monteiro and Follows 2012; Yoshikawa et al. 2013; Zamora et al. 2009). These processes are capable of reducing the accuracy of N^*.

Another method to estimate the content of denitrification derived from excess N_2 has been developed based on comparison of the dissolved N_2/Ar ratio in the water mass in and out of the denitrification regions (Codispoti 2007; Devol et al. 2006; Shigemitsu et al. 2013a). The observations of N_2/Ar have already been used in the three ODZs to estimate water-column denitrification at depths above ~1,000 m (Chang et al. 2010; Devol et al. 2006; DeVries et al. 2012). However, the dissolved N_2/Ar is sensitive not only to the denitrification process, but also physical processes, e.g., lower atmospheric pressure, rapid cooling and air injection by bubbles (Hamme and Severinghaus 2007). Hamme and Emerson (2013) reported that both net denitrification and bubble injection are the most likely effects capable of causing large changes in the dissolved N_2/Ar ratio, because the N_2/Ar ratio in the air is almost double the ratio in seawater. Regarding the constraint of excess N_2 derived from denitrification, Shigemitsu et al. (2013a) proposed a new tracer N_2^* based on N_2 and Ar in the denitrification region. However, since with this method it is difficult to determine the excess N_2 produced during denitrification caused by physical processes, only this method could not estimate the content of denitrification in the continental marginal sea.

The Okhotsk Sea (OS) is a subpolar marginal sea in the western North Pacific and the southernmost sea ice production area in the northern hemisphere. The densest water ventilating in the North Pacific region originates over the northwestern continental shelf of the OS (Kitani 1973). This water is called the dense shelf water (DSW, σ_θ = 26.7–27.0, where σ_θ is the potential density, Nakatsuka et al. 2002, 2004), which is produced by brine rejection during sea ice formation (Kitani 1973). The DSW penetrates into the intermediate depths to join with the OS intermediate water (OSIW σ_θ = 26.8–27.4, Yamamoto et al. 2002; Yamamoto-Kawai et al. 2004). The OSIW is transported into the North Pacific intermediate water (NPIW). The NPIW is widely distributed over the North Pacific, which influences the climate of the North Pacific. This water contains a large amount of anthropogenic CO_2 (e.g., Sabine et al. 2004; Wakita et al. 2005; Watanabe et al. 2001). However, the density surface of 26.8σ_θ does not outcrop to the atmosphere within the open North Pacific, even in winter (Yasuda 1997). In addition, Yasuda (1997) found a pycnostad (referred to as the OS Mode Water) in the 26.6–27.0σ_θ density range.

Primary production in the northwestern shelf region in the OS is extremely high throughout the year, except the ice-covered season (Saitoh et al. 1996; Sorokin and Sorokin 1999). Because of the strong tidal mixing and extremely low temperature in this region, the particulate organic matter produced on the shelf is exported efficiently to the pelagic intermediate water (Nakatsuka et al. 2002). Therefore, benthic flux of organic matter is possibly high in this shelf region. Yoshikawa et al. (2006) found that there was a possibility of large benthic denitrification in the continental region of the OS based on N^* (=[NO_3^-] + [NO_2^-] + [NH_4^+] − 16[PO_4^{3-}] + 2.9) × 0.87) and the nitrogen isotopic ratio of nitrate. Furthermore, Shigemitsu et al. (2013b) indicated that Fe is also reduced in such suboxic sediments in addition to nitrate based on the high Fe/Al ratio in the same region. However, the quantification of benthic denitrification has not been evaluated.

We here try to estimate the extent of benthic denitrification in the continental shelf region quantitatively. In this study, we also used the N^* ([NO_3^-] + [NO_2^-] + [NH_4^+] − 16[PO_4^{3-}] + 2.9) × 0.87) defined in Yoshikawa et al. (2006). Because the N^* includes nitrite and ammonium, the N^* would be affected by the anammox and would not be affected by dissimilatory nitrate reduction to ammonium (DNRA). To estimate the extent of benthic denitrification in the marginal sea shelf region, we focused on the density layer (σ_θ = 26.6–27.4) in the OS producing DSW and OSIW and attempted to assess the usefulness of N_2^* with N^* as the complement for detecting benthic denitrification. The DSW produced from sea ice formation on the northwestern shelf in the OS flows out to intermediate depths along the Sakhalin coast to the south and joins with the OSIW (Matsuda et al. 2009). Yoshikawa et al. (2006) showed that N^* acts as a quasi-conservative tracer of denitrification during the OSIW formation process. No

study that detects a sedimentary denitrification originating in the shelf region using N_2 and Ar exists. The OS is one of the best regions to evaluate the usefulness of this method.

2 Materials and methods

This investigation involved sampling and analyzing 28 sites to measure concentrations of dissolved gas using gas chromatography (Fig. 1). The selected sites were located from the northwestern continental shelf in the OS to the Bussol Strait. Samples were collected in 24-l X-Niskin bottles equipped with a CTD on the R/Vs Professor Khromov and Hokko-maru during August to early in September 2007 and May 2008, covering a formation area of the intermediate water in the OS (49–55°N, 142–148°E) and in the western North Pacific (40–42°N, 145–146°E), respectively.

Samples at each station were obtained at approximately 25 layers above 2,000 m depth. The collected seawater for N_2 and Ar was directly transferred from the Niskin bottle to a 60-ml glass vial. After opening the vent of the Niskin bottle, the vessel was washed twice and overflowed with three times the volume of the vessel to avoid air contamination during the transfer procedure. For the final filling, we added 50 µl of saturated $HgCl_2$ solution to prevent biological activity: the vial was covered with a butyl rubber cap and aluminum seal, paying particular attention to assure that no air bubble contamination occurred. We preserved these vials in the dark and in a cool seawater bath. The N_2 and Ar concentrations were determined by a gas-chromatographic system with thermal conductivity detection (Tanaka and Watanabe 2007) in our laboratory. Dissolved oxygen was also determined on board using the Winkler titration method (Carpenter 1965). The analytical precisions for replicate measurements of gas concentrations were within 0.04 % for N_2 and within 0.05 % for Ar.

We have found systematic offsets in the data obtained below 1,750 m depth between the stations near the Bussol Strait (A1 and A2) and Station KNOT (data from Hamme

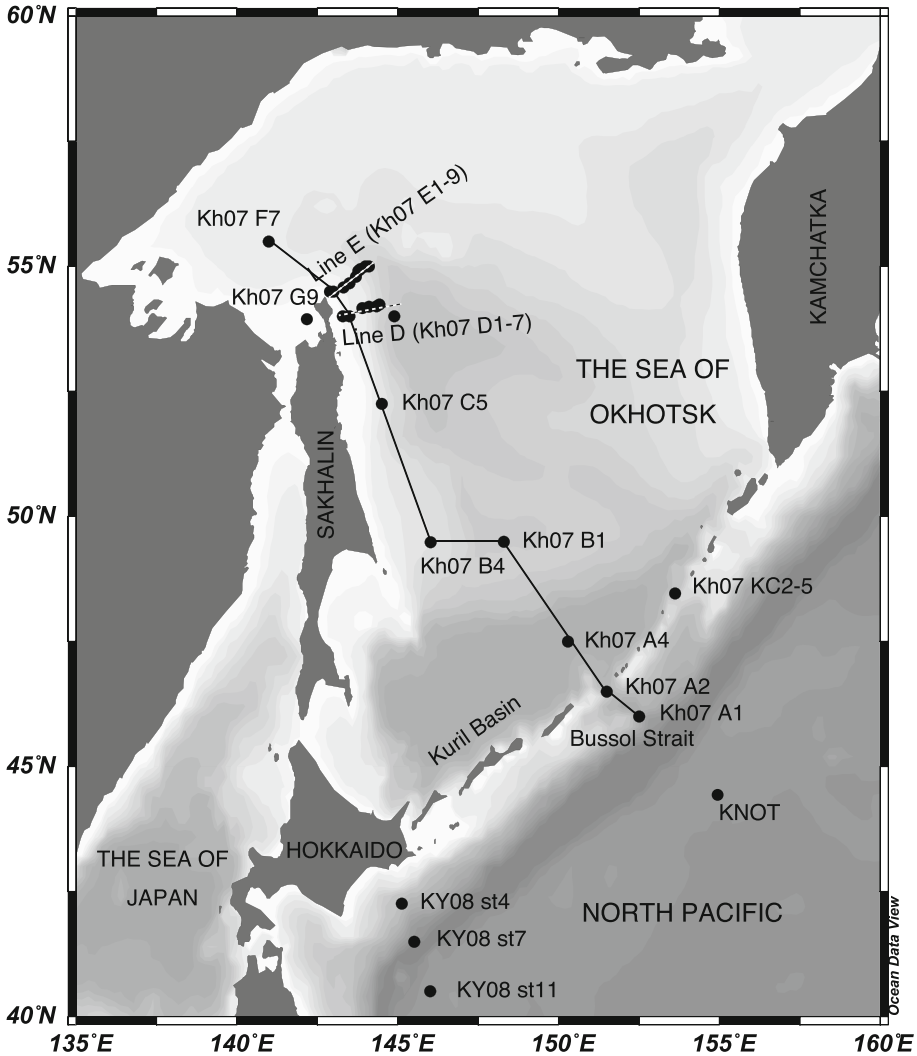

Fig. 1 Sampling points for dissolved gas and nutrients (*black filled circles*) in the Okhotsk Sea (49–55°N, 142–148°E) and the western North Pacific (40–42°N, 145–146°E). The dissolved gas samples from Station KNOT (44°N, 155°E) and the western North Pacific (KY08 st04, st07 and st11) were used as background values. The *solid line* represents *vertical sections* from the stations in Fig. 5. We used dissolved gas data from Station KNOT from R.C. Hamme's data (http://web.uvic.ca/~rhamme/download.html)

and Emerson (2002), http://web.uvic.ca/~rhamme/download.html). The average differences in temperature, salinity and density between the Bussol Strait and Station KNOT are 0.7 °C, 0.2 and 0.2 σ_θ, respectively. The oxygen concentrations in both regions were more than 60 μmol kg^{-1}. Since the above results indicated that no significant processes were affecting the Ar and N_2 concentrations, we applied the following corrections to the N_2 and Ar concentrations in the OS and the western North Pacific. We thus made corrections to the N_2 and Ar data in the OS using the following relations: $[N_2]_{meas} = [N_2]_{meas0} + 16.97$ μmol kg^{-1} and $[Ar]_{meas} = [Ar]_{meas0} + 0.87$ μmol kg^{-1}, where subscripts (meas and meas0) represented the measured concentrations after the offset corrections and raw values of our observations, respectively. In this study, we used only dissolved gas concentrations near the center of the DSW and OSIW layers between 26.6 and 27.4 σ_θ to estimate the extent of benthic denitrification that occurred in the northwestern shelf of the OS (Kitani 1973; Wakita et al. 2003, 2005; Yoshikawa et al. 2006).

3 Approach: Concepts for estimating the benthic denitrification in the Okhotsk Sea

In this study, we used the chemical tracers N_2^{ex} and N_2^* to represent the excess N_2 with N^*. One approach to estimate denitrification involves the direct measurement of the denitrification end product, i.e., the excess N_2 above the background value. There is no significant sink of N_2 gas, and the only source is denitrification in the interior of the ocean. Therefore, excess N_2 can be assumed to represent the amount of denitrification.

To estimate excess N_2, we employed a method analogous to that of Devol et al. (2006), which uses N_2/Ar ratios normalized to atmospheric equilibrium ratios:

$$N_2^{ex} = \left[(N_2/Ar)_{norm} - (N_2/Ar)_{back}\right] \times [N_2]_{sat} \times 2 \quad (1)$$

where $(N_2/Ar)_{norm}$ $(\equiv \delta N_2/\delta Ar = ([N_2]_{meas}/[N_2]_{sat})/([Ar]_{meas}/[Ar]_{sat}))$ is the ratio normalized to the atmospheric equilibrium ratio within the denitrifying waters of the ODZs, $(N_2/Ar)_{back}$ is the normalized ratio predicted for a parcel of water outside the denitrifying zone with the same density, $[N_2]_{sat}$ is the atmospheric equilibrium saturation of N_2 predicted from θ and S, and the factor of 2 converts to units of μM for monoatomic N.

Another method for estimating excess N_2 uses N_2^*, which has been developed recently (Shigemitsu et al. 2013a) as follows:

$$N_2^* = [N_2]_{meas} - \left([N_2]_{sat}/[Ar]_{sat}\right) \times [Ar]_{meas} \quad (2)$$

As mentioned above, since N_2^{ex} largely depended on the $(N_2/Ar)_{back}$ value in Eq. (1), we also used N_2^* with the assistance of multiple linear regression analysis (MLRA) to clarify the influence of denitrification and physical processes on N_2^* in this region. We considered the following factors to affect N_2^*: denitrification (J_{den}), bubble injection (J_{air}), change of solubility by rapid cooling (J_{cool}) and change of atmospheric air pressure (J_{pres}). In this study, because N_2 and Ar are similarly affected by J_{pres}, the influence of J_{pres} could be ignored.

We assumed that the observed N_2^* can be categorized into the fractions affected by J_{den}, J_{cool} and J_{air} and used MLRA to fit the data to the following equation:

$$N_2^* = a_0 + a_1 \times J_{den} + a_2 \times J_{air} + a_3 \times J_{cool} \quad (3)$$

where a_0, a_1, a_2 and a_3 are the partial regression coefficients. We here used the observed N^* values (μmol kg^{-1}) as the proxy for J_{den}, the combinations of the difference between observed and saturated Ar values (ΔAr, $[Ar]_{meas} - [Ar]_{sat}$) and the atmospheric mixing ratio of N_2 to Ar ($\chi_c = 78.084/0.934$) for J_{air}, and the difference between the potential temperature (θ) and reference temperature (T_{ref}) defined as freezing temperature at the surface for J_{cool}, namely, we have:

$$J_{den} = N^* \quad (4)$$

$$J_{air} = \Delta Ar \times \chi_c \quad (5)$$

and

$$J_{cool} = \theta - T_{ref} \quad (6)$$

In the MLRA analysis, we selected the candidate models using all possible combinations of the three explanatory variables, i.e., seven models. We selected the best model using the Akaike information criterion (AIC, Akaike 1973) as follows:

$$AIC = -2 \times L_M + 2 \times k \quad (7)$$

where L_M is the maximized log likelihood and k is the number of parameters for each model. More explanatory variables typically induce less deviation from the observed values. However, using explanatory variables in excess, we will have an instable model. The best model should include a combination of less explanatory variables and less deviation from the observed values. Using the AIC allows us to select the best model in this manner (Hilborn and Mangel 1997; Shigemitsu et al. 2010; Shimono and Kudo 2003).

4 Results and discussion

4.1 Comparison of the chemical tracers, N_2^{ex} and N_2^*

We found a significant positive correlation ($r^2 = 0.98$, $n = 45$, $p < 0.0001$; simple linear regression) between N_2^{ex} and N_2^* in the range 26.6–27.4 σ_θ Fig. 2). In Eq. (1), we

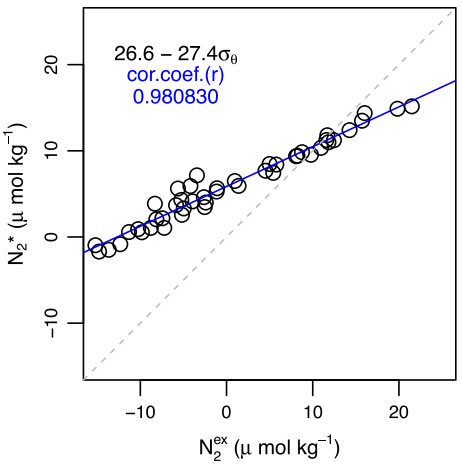

Fig. 2 The relationship between N_2^{ex} (μmol kg^{-1}) and N_2^* (μmol kg^{-1}) in the intermediate water (26.6–27.4 σ_θ) in the Okhotsk Sea. The *dashed line* represents the 1:1 line: the *solid line* shows a simple linear regression based on all our data (*open symbols*), ($y = 5.68 + 0.47x$; $r = 0.99$)

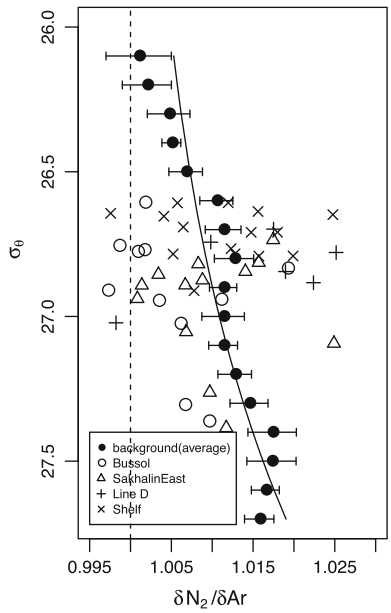

Fig. 3 Profiles of $\delta N_2/\delta Ar$ in the Okhotsk Sea and throughout the western North Pacific versus σ_θ. *Open circles* denote samples near the Bussol Strait (A1, A2, A4 and KC2-5), *triangles* denote samples from the east of Sakhalin (B1, B4 and C5), *pluses* denote samples from Line D, and *crosses* denote samples from the northwestern shelf region. *Closed circles* denote average values outside the denitrifying zone of the OS (KY08 st4, st7, st11 and KNOT). Also shown is the best fit line for $\delta N_2/\delta Ar$ in waters outside the denitrifying zone $(N_2/Ar)_{back}$. *Error bars* represent standard errors in the range of 0.001–0.004

determined $(N_2/Ar)_{back}$ using the curve fitted to $\delta N_2/\delta Ar$ observations in the western North Pacific outside of the OS [i.e., $(N_2/Ar)_{back} = 0.010\sigma_\theta^3 - 0.791\sigma_\theta^2 + 21.629\sigma_\theta - 196.062$ in Fig. 3]. Although there were large and systematic variations in the hydrographic variables (e.g., O_2 and NO_2^-) at the three stations in the western North Pacific (KY08 st4, st7 and st11), the $\delta N_2/\delta Ar$ values for the these stations did not appreciably differ. Moreover, the $\delta N_2/\delta Ar$ values were approximately 1.000 at the surface and increased to 1.020 ± 0.002 (standard error) with depth. However, since the N_2^{ex} method can be a tracer of denitrification only when there is no change in Ar concentration from the background and observed values (Codispoti 2007), it is difficult to use as an appropriate tracer for denitrification in the OS. Because the DSW is modified at the air-sea interface, the gas exchange and cooling alter both the Ar and N_2 concentrations. Therefore, we used N_2^*, which is more useful to discuss the effects of denitrification, air injection and rapid cooling on excess N_2 because the estimate of N_2^{ex} largely depended on the $(N_2/Ar)_{back}$ value.

4.2 Model selection by AIC

In the case that a correlation among the explanatory variables in a multiple regression model is high, the multicollinearity problem may occur (Graham 2003). Confounding in the regression is typically represented as a multicollinearity, for which deleterious effects on the interpretation of the regression coefficients are well known (e.g., Van Sickle 2013). The explanatory variables were screened for multicollinearity as one of the assumptions in the MLRA. Multicollinearity in the MLRA was studied by examining the tolerance, which is a statistic used to determine how much the independent variables are linearly related to one another. The tolerance is calculated as $1 - R^2$ (R^2 is the multiple coefficient of determination) for an independent variable when it is predicted by the other independent variables already included in the analysis. The higher the intercorrelation of the independent variables, the closer the tolerance is to 0. Generally,a tolerance less than 0.2 indicates a multicollinearity problem and provides an increase in the standard error of the regression coefficients (Hart and Sailor 2009; Rawlings et al. 1998). To avoid this problem, we verified the combinations of the explanatory variables having a high correlation. The correlation of J_{air} and J_{cool} (0.66) was slightly high compared to the other combinations (Table 1). However, the tolerance values for all variables in our MLRA were greater than 0.2. Therefore, there were no multicollinearity problems between our explanatory variables. In our study, we used all possible explanatory variables, J_{den}, J_{air} and J_{cool}, in the MLRA.

To clarify the amount of denitrification occurring in the northwestern shelf of the OS, we compared the results of seven models (Table 2) and evaluated N_2^* between 26.6 and 27.4 σ_θ using Eqs. (3)–(7). The best model was Model 1 because it has the smallest AIC for J_{den} and J_{air} (Table 2)

($R = 0.66$, $n = 45$, $p < 0.0001$; simple linear regression). Both denitrification and air injection primarily contributed to N_2^* in this region. Because our explanatory variables had different units, we evaluated which have a larger effect on N_2^* by using each standardized data set. We found that the largest effect was for J_{den} followed by J_{air} based on the standard partial regression coefficient (a_i', $i = 0$–3) and that a_1' and a_2' were −0.51 and −0.27, respectively.

4.3 Evaluation of the combination of N_2^* with N^* as a quasi-conservative tracer for benthic denitrification on the continental shelf

In order to evaluate the amount of denitrification by using N_2^* and N^*, it is necessary to validate the extent of N_2^* dynamics as a conservative property. In the relationship between N_2^* and potential temperature of the OSIW, we found a moderate linear relationship between the N_2^* and θ for 26.6–27.4 σ_θ in this region ($r = -0.55$, $n = 42$, $p < 0.0001$; simple linear regression), indicating that N_2^* may act as a quasi-conservative tracer for the OSIW formation process.

Plots for the Kuril Basin and Bussol Strait areas (stations A1, A2, A4 and B1) were distributed almost below the regression line (open circles in Fig. 4) because of the entrainment of low N_2^* waters from the upper layer by active tidal mixing. The other data below the regression line were the shallow layer (<75 m depth) except the deepest layer over the northwestern shelf. In this shallower

Table 1 Correlation coefficients between explanatory variables and tolerance values used for the analysis

	J_{den}	J_{air}	J_{cool}	Tolerance
J_{den}	1	0.39	0.39	0.82
J_{air}		1	0.66	0.54
J_{cool}			1	0.54

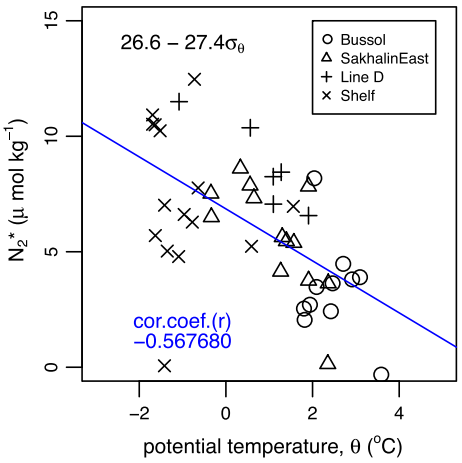

Fig. 4 Relationship between the calculated N_2^* (μmol kg^{-1}) and θ between 26.6 and 27.4 σ_θ. The *solid line* denotes the regression line ($y = 7.20-1.43x$; $r = -0.55$)

Table 2 Multiple correlation coefficient (R), number of parameters (k), maximized log likelihood (L_M), Akaike information criterion (AIC), standard partial regression coefficients [a_i' ($i = 0$ to 3)] and partial regression coefficients [a_i ($i = 0$–3)] from seven models used in this study

Model	a_0'	a_1' (J_{den})	a_2' (J_{air})	a_3' (J_{cool})	R	k	L_M	AIC
For estimating standard partial regression coefficients								
Model1	0.00	−0.51	−0.27	–	0.66	4	−50.4	108.7
Model2	0.00	−0.52	0.07	−0.31	0.66	5	−50.3	110.5
Model3	0.00	−0.61	–	–	0.61	3	−52.7	111.4
Model4	0.00	0.62	–	−0.12	0.62	4	−52.3	112.5
Model5	0.00	–	−0.47	–	0.47	3	−57.8	121.6
Model6	0.00	–	−0.43	−0.05	0.47	4	−57.8	123.5
Model7	0.00	–	–	−0.34	0.35	3	−60.6	127.2
Model	a_0	a_1 (J_{den})	a_2 (J_{air})	a_3 (J_{cool})	R	k	L_M	AIC
For estimating partial regression coefficients								
Model1	−0.34	−1.09	−2.38	–	0.66	4	−46.4	247.2
Model2	−0.71	−1.11	−2.73	0.20	0.66	5	−46.4	249.0
Model3	−0.67	−1.31	–	–	0.61	3	−49.1	249.8
Model4	0.10	−1.21	–	−0.36	0.62	4	−48.4	250.9
Model5	4.64	–	−4.12	–	0.47	3	−53.5	260.0
Model6	4.86	–	−3.81	−0.16	0.47	4	−53.4	261.9
Model7	6.78	–	–	−1.02	0.35	3	−56.4	265.6

The standard partial regression coefficients were calculated using partial regression coefficients from each standardized data set

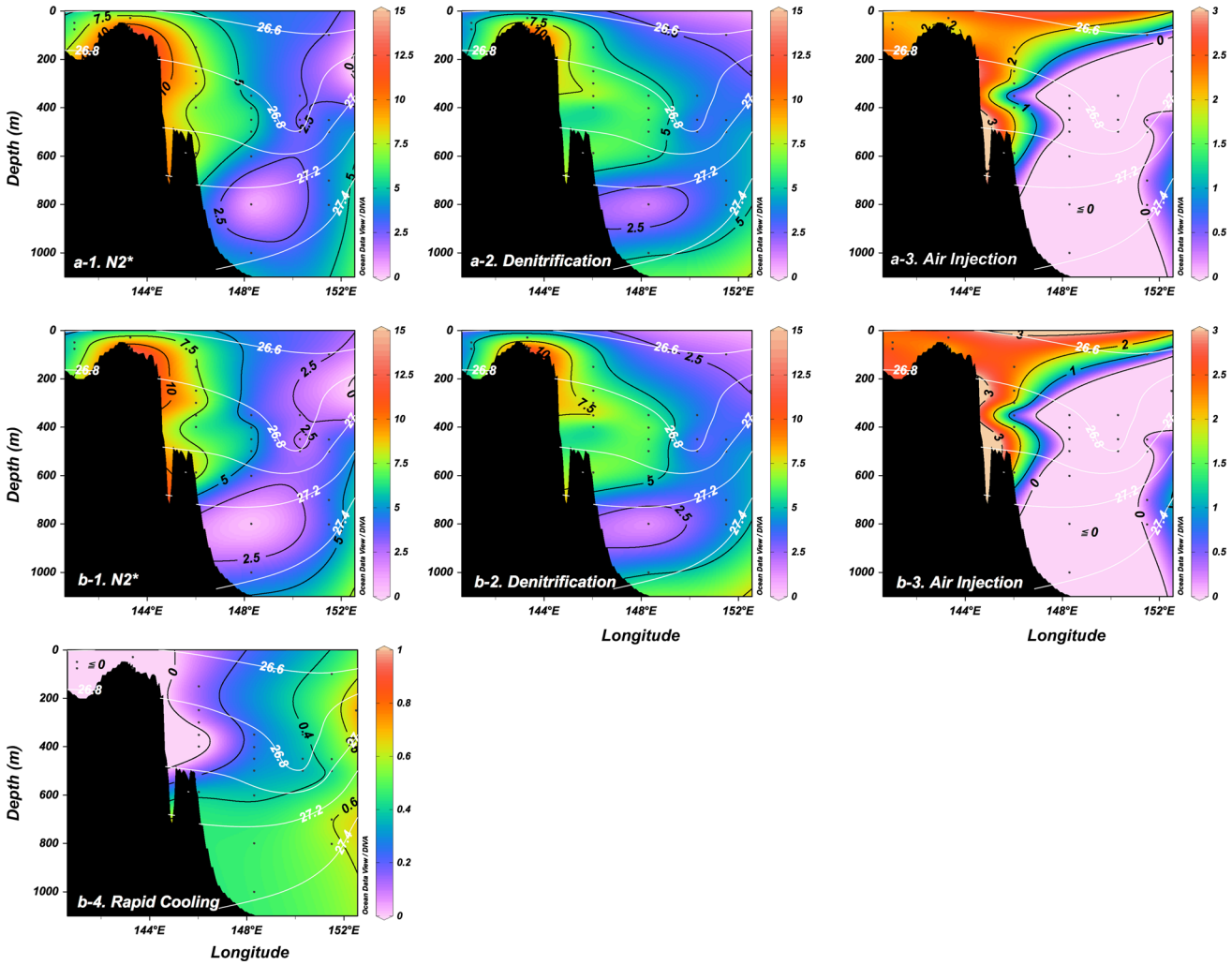

Fig. 5 Vertical cross sections of N_2^*, denitrification, air injection and rapid cooling from the northwestern shelf (140°E) to the Bussol Strait, east of Sakhalin (153°E) (*the solid line* in Fig. 1) in **a** Model 1 and **b** Model 2; **a-1** and **b-1** N_2^*, **a-2** and **b-2** denitrification, **a-3** and **b-3** air injection, **b-4** rapid cooling. All units were μmol kg^{-1}. White contour lines indicate density surfaces with *thin lines* (contour interval $0.2\sigma_\theta$). The *shading color* indicates the calculated values of each property. Ocean Data View was used to draw these figures (Schlitzer 2001)

layer, the O_2 concentration was higher than the oxygen deficient condition (<4 μmol/kg), indicating that denitrification in the water column did not occur. Furthermore, the DSW may flow out of the shelf by the gravity current along the slope and/or a western boundary current (e.g., Nakatsuka et al. 2002; Ohshima et al. 2002). Therefore, these plots may include only physical effects and consequently be lower than the regression line.

On the other hand, plots above the regression line may be due to vertical transport of high N_2^* waters; benthic denitrification occurred in the east Sakhalin sediment and northwestern shelf, because the intermediate water in this study includes the layer below the DSW (>27.0 σ_θ). This relationship of N_2^* vs. θ suggests that N_2^* at intermediate depths was not essentially changed, i.e., N_2^* levels were not affected by regeneration and the high N_2^* signature in DSW is not modified by in situ denitrification or regeneration during the formation process of OSIW and its pathways. Moreover, our finding demonstrates that N_2^* acts as a quasi-conservative tracer for the benthic denitrification.

Therefore, since both N_2^* and N^* act as a quasi-conservative tracer in the DSW, $a_1 \times J_{\mathrm{den}}$ in the MLRA acts conservatively in this layer. Thus, we concluded that the combination of N_2^* and N^* is useful to estimate a benthic denitrification in the OS.

4.4 Estimate of denitrification, air injection and rapid cooling using MLRA and AIC

Using N_2^* along with N^*, ΔAr and θ in the MLRA [Eqs. (3)–(6)], we estimated contributions of denitrification, air injection and rapid cooling to excess N_2 for the first time. By multiplying the partial regression coefficients [a_i (i = 0–3) in Table 2] by each explanatory variable value,

we can estimate the contribution of each explanatory variables as follows.

In the best Model 1, the obtained partial regression coefficient, a_1 for J_{den} was −1.09 (Table 2). We estimated the benthic denitrification in this intermediate water to be approximately 5.6 ± 2.4 μmol kg^{-1} (SD) from the $a_1 \times J_{den}$ values (Fig. 5a-1). In the same water, the observed N^* value was −5.1 ± 2.2 μmol kg^{-1}. The N^* value was approximately 2.6 ± 1.1 μmol kg^{-1} converted to N_2 yield during denitrification. These results demonstrate that excess N_2 calculated by using N_2^* along with N^* was found to be at least twice N^* alone, which agrees with the difference between N_2^{ex} and N^* in the Arabian Sea (Devol et al. 2006). What cause the difference in denitrification between excess N_2 and N^* in this region?

In the Arabian Sea, Devol et al. (2006) deduced from previous studies that several possible mechanisms increase the N_2 yield during denitrification: (1) oxidation of the ammonium regenerated during water-column denitrification to N_2, (2) contributions of N_2 resulting from processes taking place within the sediments in contact with the ODZ waters, (3) the high N:P ratio material produced during N_2 fixation or (4) denitrification fueled by non-Redfield organic matter such as preferential degradation of proteins, and (5) other reactions between metals, iodine and various N species that lead to N_2 production.

First, N^* in this study would be affected by anammox and would not be affected by DNRA, in common with N_2^*, because the N^* includes nitrite and ammonium. The rate of DNRA is three orders of magnitude lower than denitrification and anammox and is therefore insignificant in the nitrogen cycle (Crowe et al. 2012). Second, in the most intermediate water of the OS, the oxygen concentration was larger than the oxygen deficient condition (<4 μmol kg^{-1}, Codispoti et al. 2005). Third, N_2 fixation does not occur in the high-latitude OS, which is outside the habitat range of nitrogen fixers (Capone et al., 1997). Therefore, since the cases of (1)–(3) can be ignored, although we have no data about the case of (5), (4) could possibly result in most of the increases in the N_2 yield during denitrification in this study.

The N^* is a useful tracer for denitrification and N_2 fixation, and terrestrial and atmospheric inputs, but in the OS, it is possible to under/overestimate quantification of benthic denitrification by N^* alone. That is, there are possible mechanisms to increase/decrease the N^* in this region: dissolved organic nitrogen (DON) input from the Amur River and phosphate elution from sediments.

During early sedimentary diagenesis, particulate organic N is hydrolyzed to DON by bacterial hydrolytic enzymes, which can increase the N^*. A large fraction of DON is ultimately remineralized to ammonium (NH_4^+). In the presence of O_2, a portion of the regenerated NH_4^+ is oxidized to NO_3^- (nitrification) before it can escape from the sediments. This NO_3^- may in turn be used as a terminal electron acceptor by denitrifying bacteria producing gaseous forms of N (coupled nitrification–denitrification) (Lehmann et al. 2007; Thibodeau et al. 2010).

Under anaerobic sediment conditions, phosphate may also be eluted from the sediment (e.g., Sundby et al. 1992), which can decrease the N^*. Yoshikawa et al. (2006) showed that the DSW reflects not only sedimentary denitrification, but also phosphate elution from sediment from relationships between apparent oxygen utilization and phosphate concentration and nitrate concentration.

Therefore, the best way to estimate a benthic denitrification in this region is to make up for each other complementarily N_2^* and N^*. The physical processes are a disadvantage for N_2^*. The phosphate elution, DON input from the river and remineralization with the non-Redfield ratio are a disadvantage for N^*. On the other hand, the advantage of N_2^* is independent of the Redfield ratio, and it can directly estimate the end product of denitrification as excess N_2 if there are unknown biological processes. The advantage of N^* is to be used as an index of denitrification including anammox and N_2 fixation.

On the other hand, the obtained partial regression coefficient, a_2, for J_{air} was −2.38 (Table 2), and the average air injection value in the intermediate water was 0.8 ± 1.3 μmol kg^{-1} (Fig. 5a-2). The maximum air injection (ca. 2.4 μmol kg^{-1}) was found at approximately 26.7σ_θ in this region. Note that the air injection values should not be represented strictly as only air injection, but also as other physical effects—rapid cooling, heating, slow gas exchange and mixing of water masses—because the ΔAr used in J_{air} includes effects of all processes resulting in disequilibrium in the Ar concentration. However, it is difficult to estimate ΔAr only due to air injection. Therefore, as we mentioned above, we confirmed how much the independent variables are linearly related to one another by examining the tolerance. Since the tolerance values for all variables in our MLRA were greater than 0.2, our analysis may be insensitive to this error. Craig and Weiss (1971) found that the mean N_2 saturation anomaly due to air injection was 1.9 % in Pacific Deep Water. However, compared with the maximum N_2 concentration due to air injection predicted by Model 1, approximately <1 %, only half the air injection is predicted with the model. The unexpectedly low value of air injection may be caused by sea ice formation when DSW originates. When forming the dense shelf water in the wintertime, the sea surface water of the OS is covered by ice because of the strong cooling from the air mass of Siberia. Therefore, the air-sea gas exchange may be weakened by the sea ice coverage, and consequently we could observe the low value of the air injection (Tanaka and Watanabe 2007). The effect of air injection is propagated into the

abyssal zone over the northwestern shelf and the surface layer of OS. Its effect disappears below 100 m in open waters (Fig. 5a-2). In the best Model 1, we found that N_2^* was very sensitive to denitrification and air injection and insensitive to rapid cooling (<0.5 μmol kg^{-1}, Fig. 5b-4) over the OS.

In the continental shelf region, more than 80 % of N_2^* was derived from the denitrification, followed in order by air injection. The N_2^* in the intermediate water in the continental shelf (except A and B stations) was 8.3 ± 2.4 μmol kg^{-1}. The benthic denitrification (a_1 - × J_{den}) was 6.8 ± 2.4 μmol kg^{-1}. The air injection (a_2 - × J_{air}) was 1.9 ± 0.4 μmol kg^{-1}. Therefore, the effect of benthic denitrification was about 80 % or more.

5 Conclusions

This study indicates the N_2^* along with N^* would be useful tracers to estimate the benthic denitrification in the OS. Most notably, this is the first study to estimate the contributions of denitrification and other factors on N_2^* separately. Our results provide compelling evidence for evaluating the benthic denitrification in the continental marginal sediments where denitrification primarily occurs (Christensen et al. 1987; Middelburg et al. 1996). However, some limitations are worth noting. Although our hypotheses were supported statistically, J_{air} cannot represent only air injection, but also represents other physical effects, and MLRA in this study can be used only when properties in the water mass behave conservatively. Future work should therefore evaluate to what extent air injection affects N_2^* in the ocean.

Acknowledgments We thank the officers and crew of R/Vs Professor Khromov, Hokko-maru, for their kind cooperation in the fieldwork. We also wish to thank T. Nakatsuka (Nagoya University) and T. Ono (Fisheries Research Agency) for useful advice. The constructive comments of two anonymous reviewers that greatly improved this submission were highly appreciated. A part of this work was supported by the Ministry of Education, Science and Culture KAKEN grants no. 22221001 (M. Wakatsuchi, Hokkaido University).

References

Akaike H (1973) Information theory and an extension of the maximum likelihood principle. In: Petrov BN, Csaki F (eds) 2nd International symposium on information theory. Publishing House of the Hungarian Academy of Sciences, Budapest, pp 268–281

Brandes JA, Devol AH, Deutsch C (2007) New developments in the marine nitrogen cycle. Chem Rev 107:577–589. doi:10.1021/cr050377t

Capone DG, Zehr JP, Paerl HW, Bergman B, Carpenter EJ (1997) Trichodesmium, a globally significant marine cyanobacterium. Science 276:1221–1229. doi:10.1126/science.276.5316.1221

Carpenter JH (1965) The Chesapeake Bay Institute technique for the Winkler dissolved oxygen method. Limnol Oceanogr 10:141–143. doi:10.4319/lo.1965.10.1.0141

Chang BX, Devol AH, Emerson SR (2010) Denitrification and the nitrogen gas excess in the eastern tropical South Pacific oxygen deficient zone. Deep-Sea Res Part I 57:1092–1101. doi:10.1016/j.dsr.2010.05.009

Christensen JP, Murray JW, Devol AH, Codispoti LA (1987) Denitrification in continental shelf sediments has major impact on the oceanic nitrogen budget. Global Biogeochem Cycles 1:97–116. doi:10.1029/GB001i002p00097

Codispoti LA (2007) An oceanic fixed nitrogen sink exceeding 400 Tg Na^{-1} vs the concept of homeostasis in the fixed-nitrogen inventory. Biogeosciences 4:233–253. doi:10.5194/bg-4-233-2007

Codispoti LA, Christensen JP (1985) Nitrification, denitrification and nitrous oxide cycling in the eastern tropical South Pacific Ocean. Mar Chem 16:277–300. doi:10.1016/0304-4203(85)90051-9

Codispoti LA, Brandes JA, Christensen JP, Devol AH, Naqvi SWA, Paerl HW, Yoshinari T (2001) The oceanic fixed nitrogen and nitrous oxide budgets: moving targets as we enter the anthropocene? Sci Mar 65:85–105. doi:10.3989/scimar.2001.65s285

Codispoti LA, Yoshinari T, Devol AH (2005) Suboxic respiration in the oceanic water column. In: del Giorgio PA, Williams PJlB (eds) Respiration in aquatic ecosystems. Oxford University Press, Oxford, pp 225–247

Coles VJ, Hood RR (2007) Modeling the impact of iron and phosphorus limitations on nitrogen fixation in the Atlantic Ocean. Biogeosciences 4:455–479. doi:10.5194/bg-4-455-2007

Craig H, Weiss RF (1971) Dissolved gas saturation anomalies and excess helium in the ocean. Earth Planet Sci Lett 10:289–296. doi:10.1016/0012-821X(71)90033-1

Crowe SA, Canfield DE, Mucci A, Sundby B, Maranger R (2012) Anammox, denitrification and fixed-nitrogen removal in sediments from the Lower St. Lawrence Estuary. Biogeosciences 9:4309–4321. doi:10.5194/bg-9-4309-2012

Devol AH, Uhlenhopp AG, Naqvi SWA, Brandes JA, Jayakumar DA, Naik H, Gaurin S, Codispoti LA, Yoshinari T (2006) Denitrification rates and excess nitrogen gas concentrations in the Arabian Sea oxygen deficient zone. Deep-Sea Res Part I 53:1533–1547. doi:10.1016/j.dsr.2006.07.005

DeVries T, Deutsch C, Primeau F, Chang B, Devol A (2012) Global rates of water-column denitrification derived from nitrogen gas measurements. Nat Geosci 5:550. doi:10.1038/ngeo1515

Eugster O, Gruber N (2012) A probabilistic estimate of global marine N-fixation and denitrification. Global Biogeochem Cycles **26**, GB4013.10.1029/2012gb004300

Galloway JN, Dentener FJ, Capone DG, Boyer EW, Howarth RW, Seitzinger SP, Asner GP, Cleveland CC, Green PA, Holland EA, Karl DM, Michaels AF, Porter JH, Townsend AR, Vörösmarty CJ (2004) Nitrogen Cycles: past, present, and future. Biogeochemistry 70:153–226. doi:10.1007/s10533-004-0370-0

Graham MH (2003) Confronting multicollinearity in ecological multiple regression. Ecology 84:2809–2815. doi:10.1890/02-3114

Gruber N (2004) The dynamics of the marine nitrogen cycle and its influence on atmospheric co_2 variations. In: Follows M, Oguz T (eds) The ocean carbon cycle and climate, Springer, Netherlands, p. 97–148

Gruber N, Sarmiento JL (1997) Global patterns of marine nitrogen fixation and denitrification. Global Biogeochem Cycles 11:235–266. doi:10.1029/97GB00077

Hamme RC, Emerson SR (2002) Mechanisms controlling the global oceanic distribution of the inert gases argon, nitrogen and neon. Geophys Res Lett **29**, 35-31-35-34. doi:10.1029/2002GL015273

Hamme RC, Emerson SR (2013) Deep-sea nutrient loss inferred from the marine dissolved N_2/Ar ratio. Geophys Res Lett 40:1149–1153. doi:10.1002/grl.50275

Hamme RC, Severinghaus JP (2007) Trace gas disequilibria during deep-water formation. Deep-Sea Res Part I 54:939–950. doi:10.1016/j.dsr.2007.03.008

Hansell DA, Olson DB, Dentener F, Zamora LM (2007) Assessment of excess nitrate development in the subtropical North Atlantic. Mar Chem 106:562–579. doi:10.1016/j.marchem.2007.06.005

Hart M, Sailor D (2009) Quantifying the influence of land-use and surface characteristics on spatial variability in the urban heat island. Theor Appl Climatol 95:397–406. doi:10.1007/s00704-008-0017-5

Hilborn R, Mangel M (1997) The confrontation: likelihood and maximum likelihood. In: Princeton University Press (ed) the ecological detective: confronting models with data, Princeton University Press, Princeton, p 131–179

Kitani K (1973) An oceanographicstudy of the OkhotskSea: particularly in regard to cold waters. Bull Far Seas Fish Res Lab 9:45–77

Landolfi A, Oschlies A, Sanders R (2008) Organic nutrients and excess nitrogen in the North Atlantic subtropical gyre. Biogeosciences 5:1199–1213. doi:10.5194/bg-5-1199-2008

Lehmann MF, Sigman DM, McCorkle DC, Granger J, Hoffmann S, Cane G, Brunelle BG (2007) The distribution of nitrate 15°N/14°N in marine sediments and the impact of benthic nitrogen loss on the isotopic composition of oceanic nitrate. Geochim Cosmochim Acta 71:5384–5404. doi:10.1016/j.gca.2007.07.025

Liu K-K, Kaplan IR (1984) Denitrification rates and availability of organic matter in marine environments. Earth Planet Sci Lett 68:88–100. doi:10.1016/0012-821X(84)90142-0

Matsuda J, Mitsudera H, Nakamura T, Uchimoto K, Nakanowatari T, Ebuchi N (2009) Wind and buoyancy driven intermediate-layer overturning in the Sea of Okhotsk. Deep-Sea Res Part I 56:1401–1418. doi:10.1016/j.dsr.2009.04.014

Middelburg JJ, Soetaert K, Herman PMJ, Heip CHR (1996) Denitrification in marine sediments: a model study. Global Biogeochem Cycles 10:661–673. doi:10.1029/96gb02562

Monteiro FM, Follows MJ (2012) On nitrogen fixation and preferential remineralization of phosphorus. Geophys Res Lett 39:L06607. doi:10.1029/2012gl050897

Nakatsuka T, Yoshikawa C, Toda M, Kawamura K, Wakatsuchi M (2002) An extremely turbid intermediate water in the Sea of Okhotsk: implication for the transport of particulate organic matter in a seasonally ice-bound sea. Geophys Res Lett **29**, 4-1-4-4. doi:10.1029/2001gl014029

Nakatsuka T, Toda M, Kawamura K, Wakatsuchi M (2004) Dissolved and particulate organic carbon in the Sea of Okhotsk: Transport from continental shelf to ocean interior. J Geophys Res **109**, C09S14. doi:10.1029/2003jc001909

Ohshima KI, Wakatsuchi M, Fukamachi Y, Mizuta G (2002) Near-surface circulation and tidal currents of the Okhotsk Sea observed with satellite-tracked drifters. J Geophys Res **107**, 16-11-16-18. doi:10.1029/2001jc001005

Rawlings JO, Pantula SG, Dickey DA (1998) Applied Regression Analysis: A Research Tool. Springer, CA

Sabine C, Feely R, Watanabe Y, Lamb M (2004) Temporal Evolution of the North Pacific CO_2 uptake rate. J Oceanogr 60:5–15. doi:10.1023/B:JOCE.0000038315.23875.ae

Saitoh S, Kishino M, Kiyofuji H, Taguchi S, Takahashi M (1996) Seasonal Variability of Phytoplankton Pigment Concentration in the Okhotsk Sea. J Remote Sens Soc Jpn 16:172–178. doi:10.11440/rssj1981.16.172

Schlitzer R. (2001) Ocean Data View. Available at: http://www.awi-bremerhaven.de/GEO/ODV

Shigemitsu M, Watanabe Y, Yamanaka Y, Kawakami H, Honda M (2010) Relationship between sinking organic matter and minerals in the shallow zone of the western Subarctic Pacific. J Oceanogr 66:697–708. doi:10.1007/s10872-010-0057-1

Shigemitsu M, Gruber N, Oka A, Tanaka SS, Yamanaka Y (2013a) Potential use of N_2^* as a constraint on the oceanic fixed nitrogen budget. In: The oceanographic Society of Japan, Fall meeting in 2013, Sapporo, Sept. 17–21, p 208

Shigemitsu M, Nishioka J, Watanabe YW, Yamanaka Y, Nakatsuka T, Volkov YN (2013b) Fe/Al ratios of suspended particulate matter from intermediate water in the Okhotsk Sea: implications for long-distance lateral transport of particulate Fe. Mar Chem 157:41–48. doi:10.1016/j.marchem.2013.07.003

Shimono Y, Kudo G (2003) Intraspecific variations in seedling emergence and survival of potentilla matsumurae (rosaceae) between alpine fellfield and snowbed habitats. Ann Bot 91:21–29. doi:10.1093/aob/mcg002

Sorokin YI, Sorokin PY (1999) Production in the Sea of Okhotsk. J Plankton Res 21:201–230. doi:10.1093/plankt/21.2.201

Sundby B, Gobeil C, Silverberg N, Mucci A (1992) The phosphorus cycle in coastal marine sediments. Limnol Oceanogr 37:1129–1145

Tanaka SS, Watanabe YW (2007) A high accuracy method for determining nitrogen, argon and oxygen in seawater. Mar Chem 106:516–529. doi:10.1016/j.marchem.2007.05.005

Thibodeau B, Lehmann MF, Kowarzyk J, Mucci A, Gélinas Y, Gilbert D, Maranger R, Alkhatib M (2010) Benthic nutrient fluxes along the Laurentian Channel: impacts on the N budget of the St. Lawrence marine system. Estuar Coast Shelf Sci 90:195–205. doi:10.1016/j.ecss.2010.08.015

Van Sickle J (2013) Estimating the risks of multiple, covarying stressors in the National Lakes Assessment. Freshw Sci 32:204–216. doi:10.1899/11-050.1

Wakita M, Watanabe YW, Watanabe S, Noriki S, Wakatsuchi M (2003) Oceanic uptake rate of anthropogenic CO_2 in a subpolar marginal sea: the Sea of Okhotsk. Geophys Res Lett 30:2252. doi:10.1029/2003gl018057

Wakita M, Watanabe S, Watanabe YW, Ono T, Tsurushima N, Tsunogai S (2005) Temporal change of dissolved inorganic carbon in the subsurface water at Station KNOT (44°N, 155°E) in the western North Pacific subpolar region. J Oceanogr 61:129–139. doi:10.1007/s10872-005-0026-2

Watanabe YW, Ono T, Shimamo A, Sugimoto T, Wakita M, Watanabe S (2001) Probability of a reduction in the formation rate of the subsurface water in the North Pacific during the 1980s and 1990s. Geophys Res Lett 28:3289–3292

Weber TS, Deutsch C (2010) Ocean nutrient ratios governed by plankton biogeography. Nature 467:550–554. doi:10.1038/nature09403

Yamamoto M, Watanabe S, Tsunogai S, Wakatsuchi M (2002) Effects of sea ice formation and diapycnal mixing on the Okhotsk Sea intermediate water clarified with oxygen isotopes. Deep-Sea Res Part I 49:1165–1174. doi:10.1016/S0967-0637(02)00032-8

Yamamoto-Kawai M, Watanabe S, Tsunogai S, Wakatsuchi M (2004) Chlorofluorocarbons in the Sea of Okhotsk: ventilation of the intermediate water. J Geophys Res **109**, C09S11. doi:10.1029/2003JC001919

Yasuda I (1997) The origin of the North Pacific Intermediate Water. J Geophys Res 102:893–909. doi:10.1029/96JC02938

Yoshikawa C, Nakatsuka T, Wakatsuchi M (2006) Distribution of N* in the Sea of Okhotsk and its use as a biogeochemical tracer of the Okhotsk Sea Intermediate Water formation process. J Mar Syst 63:49–62. doi:10.1016/j.jmarsys.2006.05.008

Yoshikawa C, Coles VJ, Hood RR, Capone DG, Yoshida N (2013) Modeling how surface nitrogen fixation influences subsurface nutrient patterns in the North Atlantic. J Geophys Res 118:2520–2534. doi:10.1002/jgrc.20165

Zamora LM, Landolfi A, Oschlies A, Hansell D, Dietze H, Dentener F (2009) Atmospheric deposition of nutrients and excess N formation in the North Atlantic. Biogeosciences 6:9849–9889. doi:10.5194/bgd-6-9849-2009